

RESEARCH ARTICLE

Mechanistic studies of DepR in regulating FK228 biosynthesis in *Chromobacterium violaceum* no. 968

Yongjian Qiao¹✉, Tiantian Tong¹✉, Jiao Xue¹, Wenjing Lin¹, Zixin Deng¹, Yi-Qiang Cheng^{1,2}, Dongqing Zhu^{1*}

1 The Key Laboratory of Combinatorial Biosynthesis and Drug Discovery (Ministry of Education), Wuhan University, Wuhan, Hubei Province, China, **2** UNT System College of Pharmacy, University of North Texas Health Science Center, Fort Worth, Texas, United States of America

✉ These authors contributed equally to this work.

* Dzhu2011@whu.edu.cn



OPEN ACCESS

Citation: Qiao Y, Tong T, Xue J, Lin W, Deng Z, Cheng Y-Q, et al. (2018) Mechanistic studies of DepR in regulating FK228 biosynthesis in *Chromobacterium violaceum* no. 968. PLoS ONE 13(4): e0196173. <https://doi.org/10.1371/journal.pone.0196173>

Editor: Marie-Joelle Virolle, Universite Paris-Sud, FRANCE

Received: January 3, 2018

Accepted: April 6, 2018

Published: April 19, 2018

Copyright: © 2018 Qiao et al. This is an open access article distributed under the terms of the [Creative Commons Attribution License](https://creativecommons.org/licenses/by/4.0/), which permits unrestricted use, distribution, and reproduction in any medium, provided the original author and source are credited.

Data Availability Statement: All relevant data are within the paper and its Supporting Information files.

Funding: This work was supported by the National Natural Science Foundation of China (NSFC 81373305, NSFC 31401057) (D. Zhu) (<http://www.nsf.gov.cn/>), and by Hubei Provincial Natural Science Foundation of China (2017CFB618) (D. Zhu) (<http://www.hbstd.gov.cn/>). The funders had no role in study design, data collection and

Abstract

DepR, a LysR-type transcriptional regulator encoded by the last gene of the putative *min* operon (*orf21-20-19-depR*) located at the downstream region of the anticancer agent FK228 biosynthetic gene cluster in *Chromobacterium violaceum* No. 968, positively regulates the biosynthesis of FK228. In this work, the mechanism underlining this positive regulation was probed by multiple approaches. Electrophoretic mobility shift assay (EMSA) and DNase I footprinting assay (DIFA) identified a conserved 35-nt DNA segment in the *orf21-orf22* intergenic region where the purified recombinant DepR binds to. Quantitative reverse transcription PCR (RT-qPCR) and green fluorescent protein (GFP) promoter probe assays established that transcription of phasin gene *orf22* increases in the *depR* deletion mutant of *C. violaceum* (CvΔdepR) compared to the wild-type strain. FK228 production in the *orf22*-overexpressed strain *C. violaceum* was reduced compared with the wild-type strain. DepR has two conserved cysteine residues C199 and C208 presumed to form a disulfide bridge upon sensing oxidative stress. C199X point mutations that locked DepR in a reduced conformation decreased the DNA-binding affinity of DepR; T232A or R278A mutation also had a negative impact on DNA binding of DepR. Complementation of CvΔdepR with any of those versions of *depR* carrying a single codon mutation was not able to restore FK228 production to the level of wild-type strain. All evidences collectively suggested that DepR positively regulates the biosynthesis of FK228 through indirect metabolic networking.

Introduction

Bacterial cytokinesis is a complex process initiated by the formation of the Z ring, a dynamic structure formed of the tubulin homologue FtsZ. The *min* operon is one of the regulatory systems identified in *Escherichia coli* and most Gram negative bacteria, which prevents FtsZ polymerization near the cell poles [1–3]. The Min system comprises MinC, MinD and MinE proteins encoded by three genes organized as *minCDE* operon. The Min proteins blocks Z-

analysis, decision to publish, or preparation of the manuscript.

Competing interests: The authors have declared that no competing interests exist.

ring assembly near the poles of the cell via the spatial regulation of the FtsZ polymerization inhibitor MinC, which has activity only when bound by MinD [4, 5]. MinE dissociates the MinCD complex at midcell [6]. In *Neisseria gonorrhoeae*, the *min* operon is composed of four genes, *minCDE* and a LysR-type transcriptional regulator (LTTR) gene *oxyR*. OxyR regulates the expression of *minD* [7].

A similar organization of *minCDE-oxyR* operon was also found in *C. violaceum* No. 968 (Fig 1A), a producer of FK228, the most studied histone deacetylase inhibitor [8–11]. FK228 was approved by the FDA for the treatment of cutaneous T-cell lymphoma and peripheral T-cell lymphoma [12–14]. A 37-kb DNA region carrying a hybrid nonribosomal peptide synthetase-polyketide synthase (NRPS-PKS) gene cluster (*dep*) has been identified to be responsible for the biosynthesis of FK228 [15–18]. *depR* is located at the right boundary of the *dep* gene cluster and encodes a 312-aa protein with 60% identity and 76% similarity at amino acid sequence level to *N. gonorrhoeae* OxyR (306 aa). DepR is a positive regulator governing FK228 biosynthesis [17]. *depR* is peculiarly co-transcribed with three upstream genes *orf21-20-19*, which constitute the putative *min* operon and encode three Min proteins with 44%, 76%, and 59% identities and 61%, 86% and 81% similarities to MinC, MinD and MinE from *N. gonorrhoeae*, respectively. Deletion of *depR* severely reduced FK228 production but did not affect the transcriptional levels of the putative *min* genes [17].

In this study, we intended to delineate how DepR positively regulates FK228 biosynthesis through multiple approaches.

Materials and methods

Bacterial strains, plasmids, primers and general materials and methods

The bacterial strains and plasmids are listed in S1 Table. Primer sequences are listed in S2 Table.

Reagents and solvents were purchased from Sigma-Aldrich and were used without further purification. Restriction enzymes, T4 DNA ligase and DNA polymerase were purchased from New England BioLabs and used according to the manufacturer's specifications. Ni-NTA affinity columns were purchased from GE Healthcare. DNA primers were synthesized by TsingKe Inc., Wuhan, China.

Growth media and conditions used for *E. coli* strains and standard methods for handling *E. coli* *in vivo* and *in vitro* were as described previously [19], unless otherwise noted. All DNA manipulations were performed following standard procedures [19]. DNA sequencing was carried out at TsingKe Inc. All proteins were handled at 4 °C unless otherwise stated. Protein concentrations were determined according to the method of Bradford, using a PerkinElmer Lambda 25 UV/Vis spectrophotometer with bovine serum albumin as standard [20]. Protein purity was estimated using SDS-PAGE and visualized using Coomassie Brilliant Blue stain. For genomic DNA preparation, *C. violaceum* was cultured in Luria-Bertani (LB) medium supplemented with 200 µg/mL ampicillin at 30 °C for 2 days [15]. The methods of *C. violaceum* transformation and conjugation were as described previously [15, 21].

Expression and purification of recombinant DepR protein and DepR mutant proteins

A 939-bp DNA fragment harboring *depR* was obtained from plasmid pBMTL-3-*depR* digested with NdeI and HindIII and then ligated into the corresponding sites of pET-28a to give the expression plasmid pWHU1733 containing the *depR* gene fused to a His-tag coding sequence. Primers listed in S2 Table and a Fast Mutagenesis System kit (Transgen Biotech, Beijing,

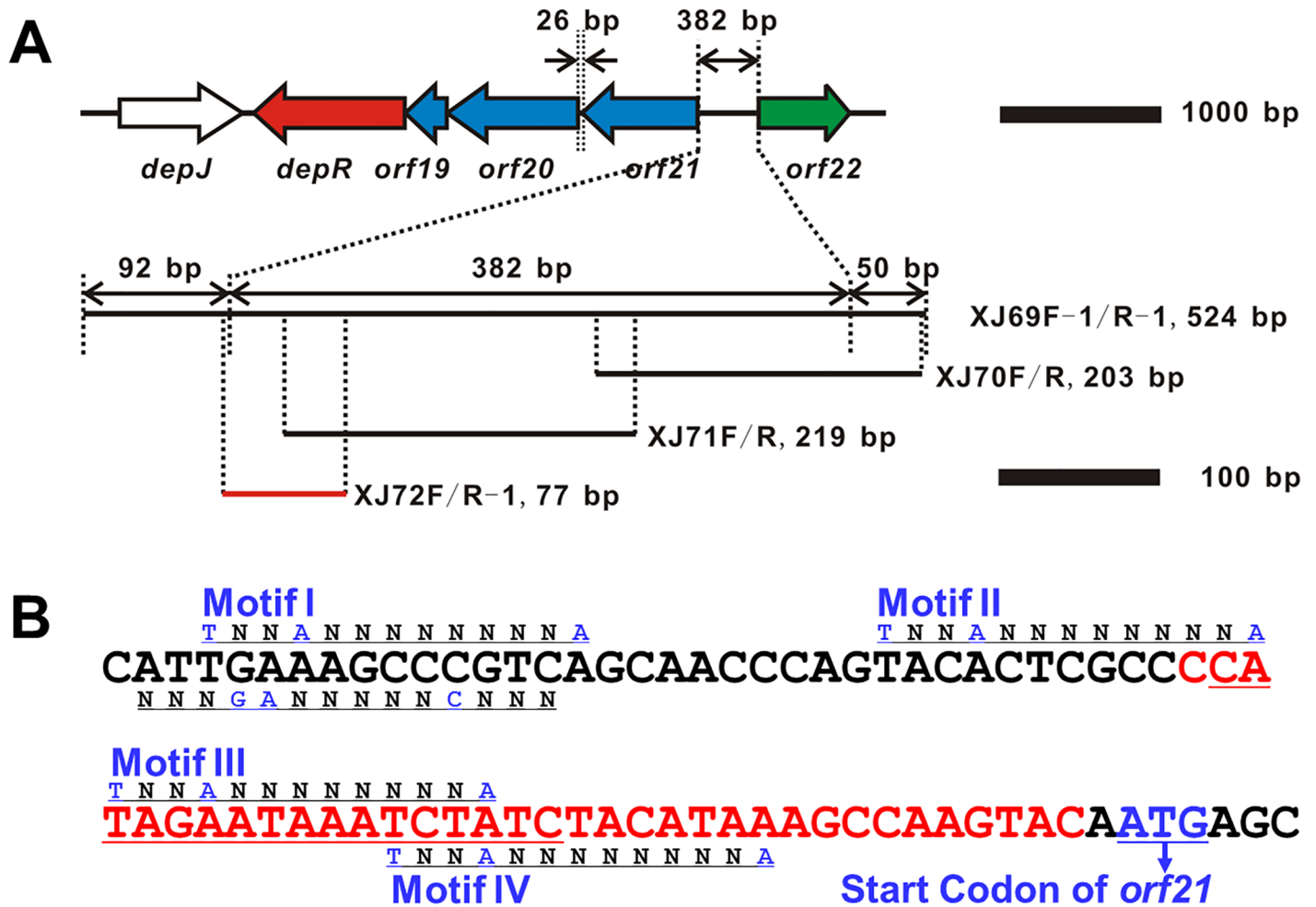


Fig 1. Genetic organization of the end of *dep* gene cluster and a conserved phasin gene (*orf22*) that encompasses a putative *min* operon (*orf21-20-19-depR*) and nucleotide sequence of DepR binding region. (A) Map of genes, intergenic regions, PCR primers and DNA fragments used in EMSAs. (B) Nucleotide sequence and motifs of a 77-bp DNA fragment to which DepR binds. Motif I-IV (TN₂AN₈A), predicted 13-bp LTTR consensus-binding motifs; N₃GAN₅CN₃, predicted RcsB consensus-binding motif; red DNA region, the exact DepR-binding site defined by DIFA; red and underlined DNA region is consistent with the characterized OxyR-binding site in *E. coli*.

<https://doi.org/10.1371/journal.pone.0196173.g001>

China) were used to introduce desired mutations into the *depR* gene on pWHU1733; mutant plasmids are listed in S1 Table. All mutations were confirmed by DNA sequencing.

The respective plasmids were introduced into *E. coli* BL21 (DE3) by transformation. The resulting recombinant *E. coli* transformant was cultured in LB medium containing 50 µg/mL kanamycin at 37 °C to an optical density at 600 nm of 0.6 to 0.8. After addition of 0.1 mM IPTG, the culture was incubated at 18 °C overnight. Cells were harvested by centrifugation and then resuspended in lysis buffer (50 mM Tris-HCl, 10% glycerol, 300 mM NaCl, 10mM imidazole, pH 7.5). After sonication, cell debris was removed by centrifugation at 20,000×g for 60 min and the supernatant was loaded onto a Ni-NTA column preequilibrated with lysis buffer. After the loaded column was washed with 20 mM imidazole in lysis buffer, proteins were eluted with elution buffer (50 mM Tris-HCl, 10% glycerol, 300 mM NaCl, 200 mM imidazole, pH 7.5). Elution fractions containing the target protein were identified by SDS-PAGE, pooled, concentrated and buffer-exchanged into storage buffer (50 mM NaH₂PO₄, 10% glycerol, pH 7.5) using a Biosharp Ultra Centrifugal filter (10 kD cut-off). The MW of protein

His₆-DepR was analyzed with a 5800 MALDI-TOF/TOF mass spectrometer (AB Sciex) by Sangon Biotech, Shanghai, China.

Sequencing of the upstream region of *orf21*

The published DNA sequence of cosmid 18 (accession no. EF210776) carrying *dep* gene cluster contains a partial *orf21* sequence. Two pairs of primers XJ69F/XJ69R and YJ85F/YJ85R were used to amplify the missing region of *orf21* and its upstream sequence from the genomic DNA of *C. violaceum* No. 968. The PCR products were sequenced, and a 1341-bp DNA sequence was obtained (accession no. MG696726).

Electrophoretic mobility shift assay (EMSA)

The binding site of DepR to the *orf21-orf22* intergenic region was determined by EMSA using the methods previously described [22–25]. Primers used to amplify putative target region DNA fragments are listed in S2 Table. Purified DepR was incubated with DNA fragments in a total volume of 20 μ L at 30 °C for 30 min. The binding buffer contained 20 mM Tris-HCl (pH 8.0), 50 mM KCl, 10 mM MgCl₂, 5% glycerol, and 0.5 mM EDTA. 0.5–1.5 mM DTT or H₂O₂ was added to the reaction mixture prior to incubation in order to change the redox status of DepR. The concentration of the dsDNA fragment was fixed at ca. 10 nM, while the concentrations of protein varied in the range of 0 to 30.7 μ M. Incubated samples were applied to 2% agarose gel and electrophoresed on ice. Gels were stained with ethidium bromide and imaged with Syngene G:BOX F3 gel doc system.

DNase I footprinting assay (DIFA)

A 130-bp promoter region of *orf21* was PCR amplified with the primer pair YJ39F/XJ72R-1, and cloned into pClone007 to generate pYJ01. DIFAs were performed similarly to the method of Wang *et al.* [26]. For preparation of fluorescent FAM labeled probes, the promoter region of *orf21* was amplified with primer pair M13F/M13R-48 (FAM) from pYJ01 using Dpx DNA polymerase (TOLO Biotech, Shanghai, China). The FAM-labeled PCR product, purified with a Wizard[®] SV Gel and PCR Clean-Up System (Promega, USA), was quantified with NanoDrop 2000C spectrometer (Thermo, USA).

For each assay, 400 ng of DNA probe was incubated with different amounts of native DepR or mutated DepR(C199S) protein in a total volume of 40 μ L at 25 °C for 30 min. A 10 μ L solution containing 0.015 unit of DNase I (Promega, USA) and 100 nmol of freshly prepared CaCl₂ was added to the reaction and further incubated at 25 °C for 1 min. Reaction was subsequently stopped by adding 140 μ L of DNase I stop solution (200 mM unbuffered sodium acetate, 30 mM EDTA and 0.15% SDS) and extracted with phenol/chloroform, precipitated with ethanol, and redissolved in 30 μ L of water. The preparation of DNA ladders, electrophoresis and data analysis were the same as described [26], except that the GeneScan-LIZ500 size standard (Applied BioSystems) was used.

Determination of promoter activity by GFP production

The promoterless *gfp* gene from pWHU1421 (provided by Dr. L. Cheng, Wuhan University, unpublished) was used as reporter gene. *gfp* was amplified with primer pair DQ132F/DQ132R and cloned into the downstream NdeI/BglII sites of T7 promoter of pACYCDuet-1 to generate pWHU3026. The 388-bp intergenic region covering the promoter of *orf21* from *C. violaceum* was amplified using the primer pair XJ79F and XJ79R, inserted into the EcoNI+NdeI sites of pWHU3026 to replace the T7 promoter, and generated pWHU3027. The 388-bp intergenic

region covering the promoter of *orf22* from *C. violaceum* was amplified using the primer pair 3T17F and 3T17R, inserted into the EcoNI+NdeI sites of pWHU3026 to replace the T7 promoter, and generated p3T11. The 525-bp intergenic region covering the promoter of *minC* from *E. coli* was amplified using the primer pair XJ80F and XJ80R, inserted into the EcoNI+NdeI sites of pWHU3026 to replace the T7 promoter, and generated pWHU3028. *E. coli* BL21(DE3) was transformed by introducing the plasmids, respectively.

The broad host-range gene expression vector pBMTL-3 was digested with BsaXI and XbaI, filled with Klenow fragment to create a blunt end, and ligated with T4 ligase to generate pYJ44 without a *lac* promoter region. The 1108-bp EcoRV/HindIII DNA fragment carrying the promoter region of *orf21* and *gfp* gene amplified from pWHU3027 with primer pair YJ81F-1/YJ80R, or the promoter region of *orf22* and *gfp* gene amplified from p3T11 with primer pair YJ82F-1/YJ80R, inserted into the corresponding sites of pYJ44 to generate pWHU3064 and pWHU3065, respectively. Each of the plasmids was transferred into *C. violaceum* wild-type strain or the *depR* mutant strain CvΔdepR using the method previously described [15, 21].

Promoter activity was measured as the rate of GFP production divided by the OD₆₀₀ of the culture at each time point [27, 28]. *E. coli* BL21 (DE3) (pWHU3028) and the negative control strain *E. coli* BL21 (DE3) (pACYCDuet-1) were cultured in LB medium containing 25 μg/mL chloramphenicol at 37 °C overnight, respectively. 2% (v/v) of the overnight culture was transferred in 20 mL fresh LB medium and was grown at 37 °C for 12 hours. Samples were withdrawn every two hours. *E. coli* BL21 (DE3) (pWHU3027, pET28a), BL21 (DE3) (pWHU3027, pWHU1733), BL21 (DE3) (p3T11, pET28a), and BL21 (DE3) (p3T11, pWHU1733) and the negative control strains *E. coli* BL21 (DE3) (pACYCDuet-1, pET28a) and BL21 (DE3) (pACYCDuet-1, pWHU1733) were cultured in LB medium containing 25 μg/mL chloramphenicol and 50 μg/mL kanamycin at 37 °C overnight, respectively. 2% (v/v) of the overnight culture was transferred in 20 mL fresh LB medium and was grown at 37 °C to an optical density at 600 nm of ca. 0.6. After the addition of 0.1 mM IPTG, the culture was further incubated at 28 °C for 12 hours. Samples were withdrawn every two hours. *C. violaceum* No. 968 (pWHU3064), CvΔdepR (pWHU3064), No. 968 (pWHU3065), and CvΔdepR (pWHU3065), and the negative control strains *C. violaceum* No. 968 (pYJ44) and CvΔdepR (pYJ44) were cultured in the fermentation medium (1% Difco nutrient broth and 1% glucose) containing 25 μg/mL chloramphenicol and 100 μg/mL ampicillin at 28 °C overnight, respectively. 1% (v/v) of the overnight culture was transferred in 20 mL fresh fermentation medium containing 25 μg/mL chloramphenicol and 100 μg/mL ampicillin and was grown at 28 °C for 72 hours. Samples were withdrawn every 8 hours or 12 hours. NanoDrop 2000C Spectrophotometer (Thermo Scientific) was used to test the optical density at 600 nm of the samples. Infinite M200 Pro (Tecan) was used to detect fluorescence of GFP (excitation/emission wavelength, 485/520).

RNA extraction and quantitative reverse transcriptase PCR (RT-qPCR)

C. violaceum wild-type and CvΔdepR were cultured in fermentation medium (1% Difco nutrient broth and 1% glucose) at 28 °C and cells were harvested at an OD₆₀₀ of 0.5–0.6 in triplicate. Total bacterial RNA was isolated using a RNeasy Mini Kit (Qiagen) according to manufacturer's instruction. RNase-free DNase (Promega, USA) was used to digest and remove DNA from RNA samples. Absence of residual DNA in RNA samples was verified by control incubations of the primer pair YJ71F and YJ71R, in which, the reverse transcriptase step was omitted did not give any PCR-amplified product of 16S rDNA. The typical PCR reaction included the initial denaturation step (94 °C, 5 min), 35 cycles of amplification (94 °C, 30 s; 60 °C, 30 s; 72 °C, 30 s), and then a final incubation (72 °C, 5 min). The quality and concentration of RNA was determined by UV/Vis spectrophotometry and by gel electrophoresis. RT-qPCR was used to

compare the expression levels of selected genes in *C. violaceum* wild-type and *CvΔdepR*, using primers listed in [S2 Table](#). Specifically, RNA was transcribed into cDNA using EasyScript One-Step gDNA Removal and cDNA Synthesis SuperMix (Transgen) according to manufacturer's instruction. qPCR was performed using AceQ qPCR SYBR Green Master Mix (Vazyme). A 7900HT Fast Real-Time PCR system (Applied BioSystems) was used to complete the reactions. The values were normalized to 16S rRNA expression for each sample. The expression levels of *orf19*, *orf21* and *orf22* in *CvΔdepR* were calculated relative to those of the wild-type strain using $\Delta\Delta C_T$ [29].

Detection and quantification of FK228 production by LC-MS

FK228 production was quantified similarly to the method previously described [15, 16]. Wild-type, mutant, and complementation strains of *C. violaceum* were cultured in 20 mL of fermentation medium with 5% (w/v) of Diaion HP-20 resins at 28 °C for 3 days. After fermentation cells and resins were collected together by centrifugation and lyophilized to dryness. Ten mL ethyl acetate was used to extract the dried mass and the organic extracts were concentrated on a rotovap. The residue was resuspended in 350 μ L methanol and 15 μ L of such organic extract was analyzed with a Thermo Scientific LTQ Orbitrap LC-MS for the detection and quantification of FK228 production.

Results

Identification of the DepR-binding site

The *depR* gene was excised from pBMTL-3-*depR* and cloned into pET28a for overexpression in *E. coli* BL21(DE3). Recombinant DepR carrying an N-terminal His₆ tag (predicted, *m/z* 36,182.21 Da) was purified to >90% purity with Ni²⁺-NTA columns ([S1A Fig](#)), which showed a subunit *M_D* by MALDI-TOF/TOF MS of *m/z* 36,043 (predicted P-Met, 36,043.35). In addition, the presence of multiple MS signals at *m/z* 72,079, 108,120 and 144,301 suggested that DepR may be present in the solution as a dimer, trimer or tetramer ([S2 Fig](#)).

The upstream region of *orf20* may contain a DepR-binding region based on the previous research on OxyR, the homologue of DepR in *N. gonorrhoeae* [7]. Initially a 401-bp DNA fragment carrying the 26-bp *orf20-orf21* intergenic region ([Fig 1A](#)) was obtained by PCR amplification using the primer pair XJ59F/XJ59R. However, EMSAs did not detect an obvious binding of the purified DepR to this stretch of DNA ([Fig 2A](#), Left). Since *depR* as the last gene of the putative *min* operon is co-transcribed with *orf21-20-19* [17], the upstream region of *orf21*, the first gene of the putative *min* operon, may contain a DepR-binding region. The published DNA sequence of cosmid 18 (accession no. EF210776) carrying the *dep* gene cluster only contains a partial 3'-*orf21* sequence, so we amplified and sequenced a 1341-bp new DNA which contains a 392-bp 5'-*orf21*, a 567-bp ORF (named *orf22* encoding a putative phasin-family protein) and a 382-bp intergenic region *orf21-orf22* ([S3 Fig](#)). EMSAs using DepR and a 524-bp DNA fragment carrying the 382-bp *orf21-orf22* intergenic region, obtained by PCR amplification using the primer pair XJ69F-1/XJ69R-1, showed a protein-DNA binding ([Fig 2A](#), Right). To further refine the actual DNA-binding target of DepR, primers were used to amplify different portions of the *orf21-orf22* intergenic region ([Fig 1A](#) and [S2 Table](#)), and the EMSA using DepR and a 77-bp DNA fragment obtained by PCR amplification using the primer pair XJ72F/XJ72R-1, showed a protein-DNA binding ([Fig 2B](#), Right). EMSAs using DepR and a 203-bp or a 219-bp DNA fragment obtained by PCR amplification using the primer pair XJ70F/XJ70R or XJ71F/XJ71R did not show any detectable protein-DNA binding ([Fig 2B](#), Left).

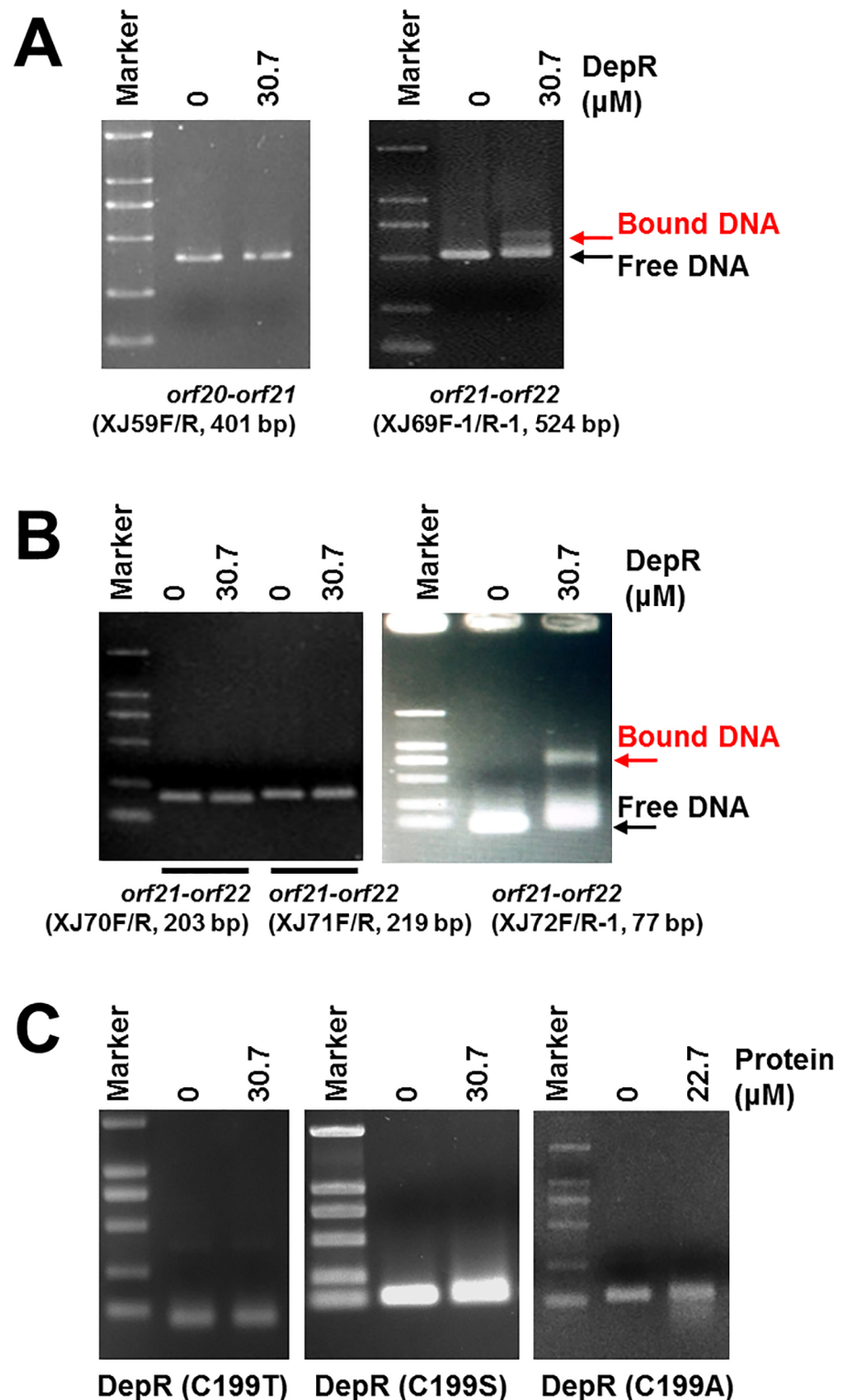


Fig 2. EMSAs of DepR with DNA fragments from the *orf22-21-20-19-depR* region. (A) EMSAs of DepR with DNA fragments harboring the intergenic region of *orf20-orf21* or the intergenic region of *orf21-orf22*. (B) EMSAs of DepR with DNA fragments covering different parts of the intergenic region of *orf21-orf22*. (C) EMSAs of three DepR mutants with target DNA fragment of DepR. Delete “Effects of DTT and H₂O₂ on the binding of DepR to target DNA fragments. (D)”.

<https://doi.org/10.1371/journal.pone.0196173.g002>

This 77-bp DNA region upstream of the start codon of *orf21* contains four 13-bp LTTR consensus-binding motifs (T-N₁₁-A) (Fig 1B, Motif I-IV). Alignment of these four 13-bp motifs showed the fourth nucleotide is also consensus (T-N₂-A-N₈-A). DIFAs in the presence of 4 μM DepR revealed that the exact DepR-binding site covered a 35-nt region (Fig 3), which is located at 36–2 nt upstream of the start codon of *orf21* (Fig 1B, red DNA region). This exact DepR-binding site harbors a 17-bp region (cATAGaaTAAATCTATC; the capital letters are consistent and the small letters are inconsistent.) (Fig 1B, red and underlined DNA region) that is also mostly consistent with the characterized OxyR-binding site (GATAGBYHWDRVCTATC) in *E. coli* [30].

Repression of the expression of phasin protein-coding gene *orf22* by DepR

The previous semi-quantitative RT-PCR results did not suggest a regulatory role of DepR on the expression of the putative *min* operon in *C. violaceum* No. 968 [17]. To probe a possible regulatory role of DepR on the expression of *orf22*, green fluorescent protein (GFP) expression assays and RT-qPCR were performed.

GFP expression assays were performed in *E. coli* firstly, since the FK228 biosynthetic genes can be expressed in *E. coli* as a heterologous host [18]. Plasmid pWHU3026 carrying a *gfp* gene was constructed to be a promoter probe vector in *E. coli*. The promoter region of *minC* in *E. coli* was amplified and replaced the T7 promoter upstream of *gfp* in pWHU3026 to yield pWHU3028 as a positive control. GFP production in *E. coli* BL21(DE3) (pWHU3028) reached 600 to 900 GFP/OD₆₀₀ throughout the 12-hour test period when it was under the control of *minC* promoter from *E. coli* (S4 Fig). Similarly, the *orf21-orf22* intergenic region was amplified by PCR and replaced the T7 promoter upstream of *gfp* in pWHU3026 in either direction to generate pWHU3027 (corresponding to the putative promoter of *orf21*, P_{*orf21*}) or p3T11 (corresponding to the putative promoter of *orf22*, P_{*orf22*}). Comparing to the negative controls of *E. coli* BL21(DE3) (pACYCDuet-1, pET28a) and BL21(DE3) (pACYCDuet-1, pWHU1733), the level of GFP under the control of P_{*orf21*} also reached ca. 800 GFP/OD₆₀₀ [Fig 4A, BL21(DE3) (pWHU3027, pET28a)], and *depR* overexpression increased the GFP production ca. 23–66% [Fig 4A, BL21(DE3) (pWHU3027, pWHU1733)]. The level of GFP under the control of P_{*orf22*} reached ca. 12,000 GFP/OD₆₀₀ [Fig 4B, BL21(DE3) (p3T11, pET28a)], significantly higher than the level of GFP promoted by P_{*orf21*}. It is interesting to note that *depR* overexpression repressed the level of GFP under the control of P_{*orf22*} ca. 30–45% (Fig 4B, BL21(DE3) (p3T11, pWHU1733)). Those results indicated that DepR activates the *orf21* promoter and represses the *orf22* promoter in the heterologous host *E. coli*.

To perform GFP expression assays in *C. violaceum*, the *lac* promoter of pBMTL-3 was deleted to generate pYJ44, and two versions of the pYJ44-derived plasmids, pWHU3064 and pWHU3065 harboring *gfp* under the control of P_{*orf21*} or P_{*orf22*}, were constructed and conjugated into No. 968 and CvΔdepR. The vector pYJ44 was also conjugated into these two strains as negative controls. Unlike the results in *E. coli*, GFP level under the control of P_{*orf21*} did not show a difference between in CvΔdepR and in the wild-type strain, which remained 400–1,400 GFP/OD₆₀₀ during the testing period (Fig 4C). The level of GFP under the control of P_{*orf22*} in *C. violaceum* reached ca. 20,000–60,000 GFP/OD₆₀₀ (Fig 4D), significantly higher one to two orders of magnitude than the level of GFP promoted by P_{*orf21*}. GFP under the control of P_{*orf22*} in CvΔdepR was ca. 15–40% higher than that in the wild-type strain (Fig 4D). According to the growth curve of *C. violaceum*, the GFP level under the control of P_{*orf22*} increased and reached a maximum in the exponential phase following by a rapid decrease, and then kept relatively stable throughout the stationary phase and decline phase.

To investigate the regulatory role of DepR by performing comparative transcriptional analysis between the wild-type and the CvΔdepR strain, RT-qPCR experiments were performed

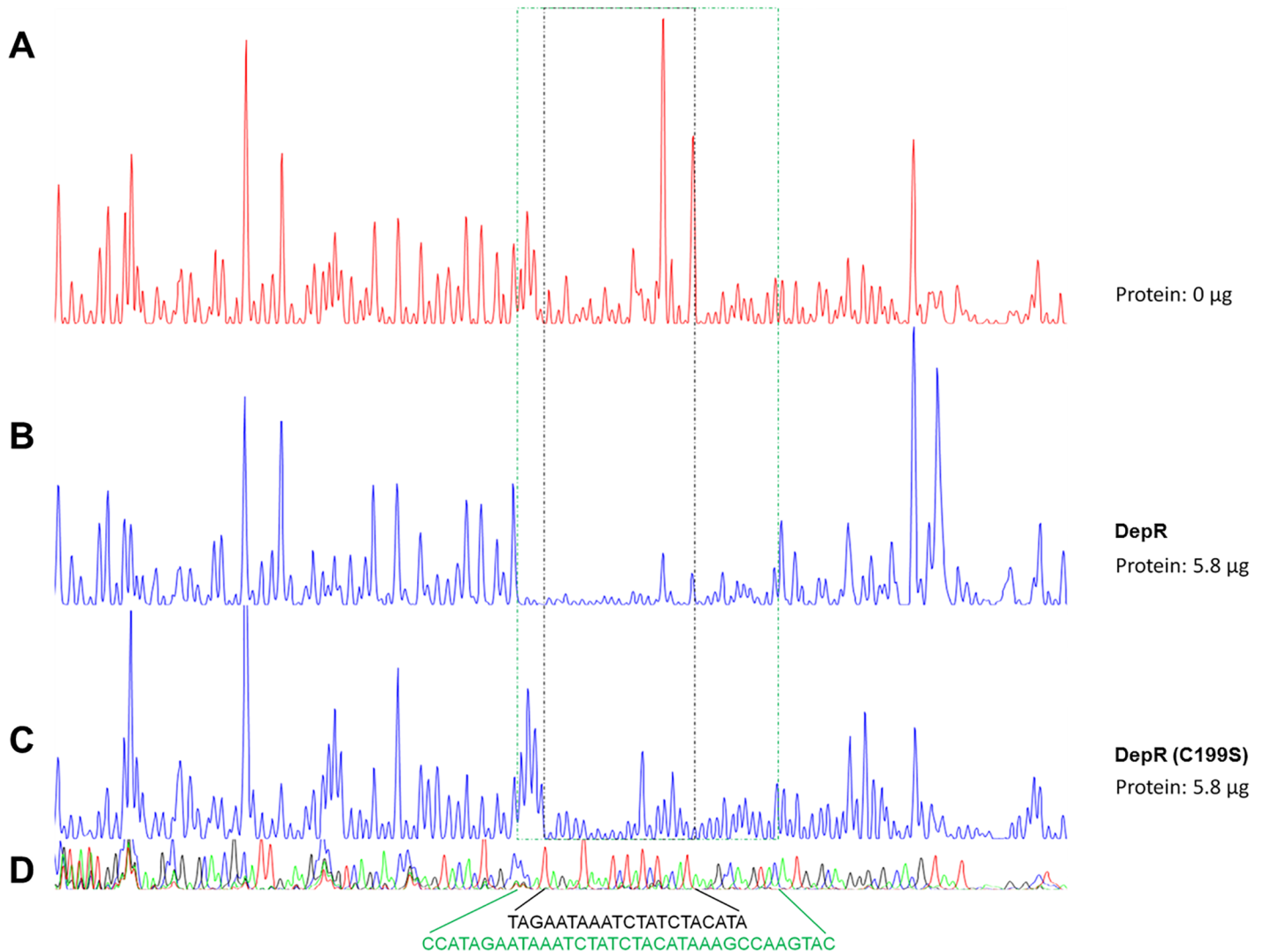


Fig 3. Identification of the exact DepR-binding sites in the *orf22-orf21* intergenic region using DIFAs. (A) The electropherogram of a reaction in the absence of protein. (B) The electropherogram of a reaction in the presence of 5.8 µg (4 µM) purified protein DepR. (C) The electropherogram of a reaction in the presence of 5.8 µg (4 µM) purified protein DepR (C199S). (D) The electropherogram of a sequencing reaction. The DNA sequences show DepR (green) or DepR (C199S) (black) binding sites.

<https://doi.org/10.1371/journal.pone.0196173.g003>

with RNA isolated from the wild-type and CvΔdepR strain grown in fermentation medium to an optical density at 600 nm of 0.5–0.6. The transcription levels of *orf19* and *orf21* in the putative *min* operon did not decrease significantly in CvΔdepR; in contrast, the transcription level of *orf22* increased ca. one fold in CvΔdepR (Fig 5). Those results indicated that DepR represses the *orf22* promoter in *C. violaceum*.

Amino acid residues important for DepR binding

OxyR, a LysR-type transcriptional regulator with two conserved cysteine residues C199 and C208, was the first discovered redox-sensitive factor that is activated by a thiol-disulfide switch [31–35]. OxyR alters its contact with DNA under oxidizing or reducing conditions. The redox status of OxyR can be manipulated by adding DTT as a reductive agent or H₂O₂ as an

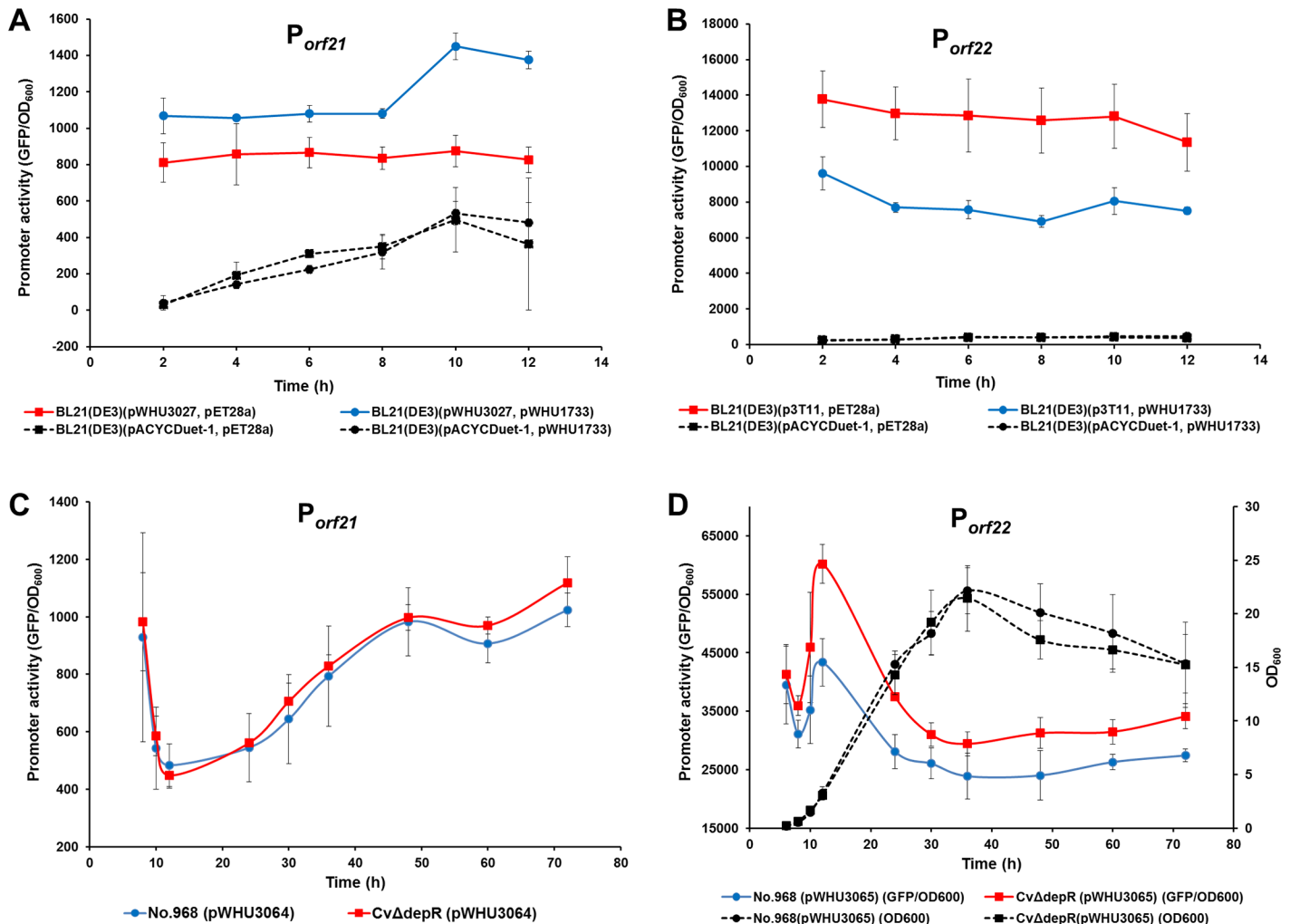


Fig 4. GFP expression assays of the promoter of *orf21* (P_{orf21}) and the promoter of *orf22* (P_{orf22}). (A) P_{orf21} in *E. coli* strain BL21(DE3); (B) P_{orf22} in *E. coli* strain BL21(DE3); (C) P_{orf21} in *C. violaceum* wild-type strain and CvΔdepR mutant strain; (D) P_{orf22} in *C. violaceum* wild-type strain and CvΔdepR mutant strain. Error bars indicate the standard deviation (n = 3).

<https://doi.org/10.1371/journal.pone.0196173.g004>

oxidative one. An OxyR (C199S) mutant locks in the reduced status, which behaves like reduced OxyR generated by using DTT [36]. The T238 residue of OxyR is buried in the core of the region containing the redox-active C199 and C208. A T238A mutation might impair the disulfide bond formation and lock the mutated protein in a reduced status [37]. D142 and R273 may locate the region of OxyR that interacts with RNA polymerase. OxyR (D142A) and OxyR (R273H) mutants no longer activate the expression of its target gene but only partially lose their DNA binding capacity [37]. On the basis of the extensively studied OxyR, we did EMSAs using purified DepR under oxidizing or reducing conditions. Sequence alignment of DepR and OxyR (GenBank, WP_001025939) was used aid in point mutants of DepR. We prepared six DepR mutants in which the selected residues correspond to the above-mentioned amino acids in OxyR. EMSAs of wild-type DepR and the DepR target DNA fragment were used as positive controls in the following EMSAs of DepR mutants.

In EMSA using native DepR and the 130-bp DNA fragment carrying the DepR target region, addition of 0.5–1.5 mM DTT resulted in less DNA binding; the bound DNA band

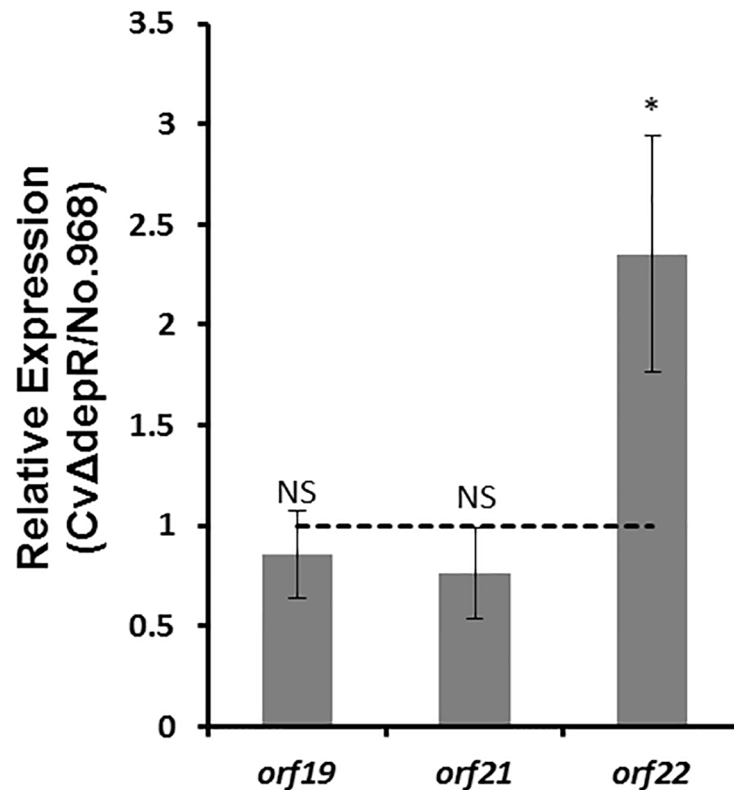


Fig 5. Effects of *depR* deletion on the expression of *orf19*, *orf21* and *orf22*. Fold changes in the expression levels of *orf19*, *orf21* and *orf22* in the exponential phase of *depR* mutant strain CvΔ*depR* as compared to the wild-type strain. Using gene specific primers, RT-qPCR on total RNA from CvΔ*depR* and the wild-type strain. Data analysis was done as described in Materials and methods. Data are mean values of results from duplicate independent experiments with error bars indicating standard deviation. Statistical significance was determined by Student's test. *, $P < 0.05$; NS, not significant. Error bars indicate the standard deviation ($n = 3$).

<https://doi.org/10.1371/journal.pone.0196173.g005>

began to disappear as the concentration of DTT increased (S6A Fig). H_2O_2 added at 0.5–1.5 mM had little or no effect on DepR-DNA binding (S6B Fig).

To precisely define the residue(s) undermining DepR-DNA binding, three point-mutated proteins, DepR (C199T), DepR (C199S) and DepR (C199A), were purified (S1A Fig), since the attack on C208 by C199 generates an intramolecular disulfide bond that drives massive conformational changes in the protein. EMSAs using the 77-bp or a 130-bp DNA fragment and those DepR (C199X) mutants showed that the bands of protein-bound DNA disappeared (Fig 2C). We carried out DIFA in the presence of 5.8 μ g (4 μ M) or 9.8 μ g (6.8 μ M) purified protein DepR (C199S) (Fig 3C, S5 Fig). The results revealed that the exact DepR(C199S)-binding site covered a 21-nt region located 33–13 nt upstream of the start codon of *orf21* (Fig 3D, the black DNA sequences). DepR (T244A) mutant was also generated and purified (S1B Fig). EMSA using DepR (T244A) and the 130-bp DNA fragment carrying the DepR target region showed that the bound DNA band was weakened compared with the positive control DepR (S7 Fig). DepR (D142A) was produced as insoluble inclusion bodies (not shown); DepR (R278A) was produced in soluble form and purified (S1B Fig). EMSA using the 130-bp DNA fragment carrying the 35-bp DepR target region according to the above DIFAs showed that DepR (R278A) lacked a DNA binding capacity (S7 Fig).

We also substituted three other conserved residues S229, T232 and R271 with alanine. DepR (R271A) was insoluble (not shown); DepR (S229A) and DepR (T232A) were soluble and

purified (S1B Fig). EMSA showed that DepR (T232A) is defective in DNA binding (S7 Fig), while EMSA using DepR (S229A) and the 130-bp DNA fragment carrying the DepR target region or a 136-bp DNA fragment as negative control exhibited unexplainable smears.

In summary, the DNA binding ability for the deduced DepR decreased compared with the purified native DepR. The T232A or R278A mutation had a negative impact on DNA binding of DepR.

Effects of point-mutations of DepR on FK228 production

Production of FK228 by Cv Δ depR is severely impaired, while complementation of *depR* restores FK228 production [17]. To delineate the effects of point-mutations of DepR on FK228 production, seven *depR* point-mutated gene variants [*depR* (C199A), *depR* (C199S), *depR* (C199T), *depR* (S229A), *depR* (T232A), *depR* (T244A), *depR* (R278A)], each encoding a soluble mutated protein in *E. coli* protein expression system, were cloned into the expression vector pBMTL-3, respectively. The pBMTL-3-based plasmids were introduced into Cv Δ depR to generate seven complementation strains (S1 Table), followed by fermentation. FK228 produced by each strain, including Cv Δ depR as a negative control and the wild-type No. 968 strain and the Cv Δ depR/pBMTL-3-*depR* complementation strain as positive controls, was quantified with LC-MS (Fig 6). Full FK228 production was not restored by complementation of Cv Δ depR with *depR* (C199X), *depR* (T232A) or *depR* (R278A) (Fig 6, red), which encodes DepR mutant lacking a DNA binding capacity according to EMSAs (Fig 2 and 2D; S7 Fig). FK228 production was restored to full level or above by complementation of Cv Δ depR with *depR* (S229A) or *depR* (T244A) (Fig 6, blue). These findings suggest that the reduced DepR cannot regulate the biosynthesis of FK228 positively and that the T232A or R278A mutation has a negative impact on the activation of DepR on FK228 production.

Discussion

Positive but indirect regulation of FK228 Biosynthesis by DepR

The previous experiments revealed that FK228 production and the transcription level of most *dep* genes, including *depABCDEFGHIH* and *depI*, decreased in the Cv Δ depR mutant, which led to the conclusion that FK228 biosynthesis is positively regulated by DepR in *C. violaceum* No. 968 [17]. According to the operon organization of *dep* gene cluster, five intergenic regions (*depL-depM*, *depM-depN*, “*depN*”-*depA*, *depH-depI*, and *depI-depJ*) and an intragenic region (“*depN*”, a pseudogene upstream of *depA*) (S8A Fig) were amplified and used in EMSAs with purified DepR. Surprisingly, EMSAs did not show any detectable protein-DNA binding (S8B Fig). Two DNA fragments from the intragenic regions of *depM* and *depA*, respectively, were amplified and tested, but no protein-DNA binding was observed in EMSAs as well (S8B Fig). Furthermore, EMSAs with reduced DepR (in the presence of DTT) also does not show any detectable protein-DNA binding (not shown). These EMSAs suggested that the FK228 biosynthetic gene cluster doesn't contain DepR-binding site.

Thailandepsins and spiruchostatins belong to the FK228-family of natural products, and their biosynthetic gene clusters (*tdp* and *spi*) have been characterized in *Burkholderia thailandensis* E264 and *Pseudomonas* sp. Q71576, respectively [38–40]. Unlike *depR*, which is located downstream of the *dep* gene cluster and encodes an OxyR-family transcriptional regulator, an AraC-family transcriptional regulator gene *tdpR* and a LysR-family transcriptional regulator gene *spiR* are located upstream of the *tdp* and *spi* gene clusters, respectively. TdpR and SpiR are not homologues of DepR according to their protein sequences. SpiR positively regulates the biosynthesis of spiruchostatin. The heterologous overexpression of DepR enhanced spiruchostatin production possibly through upregulating *spiR* expression [39]. All those results

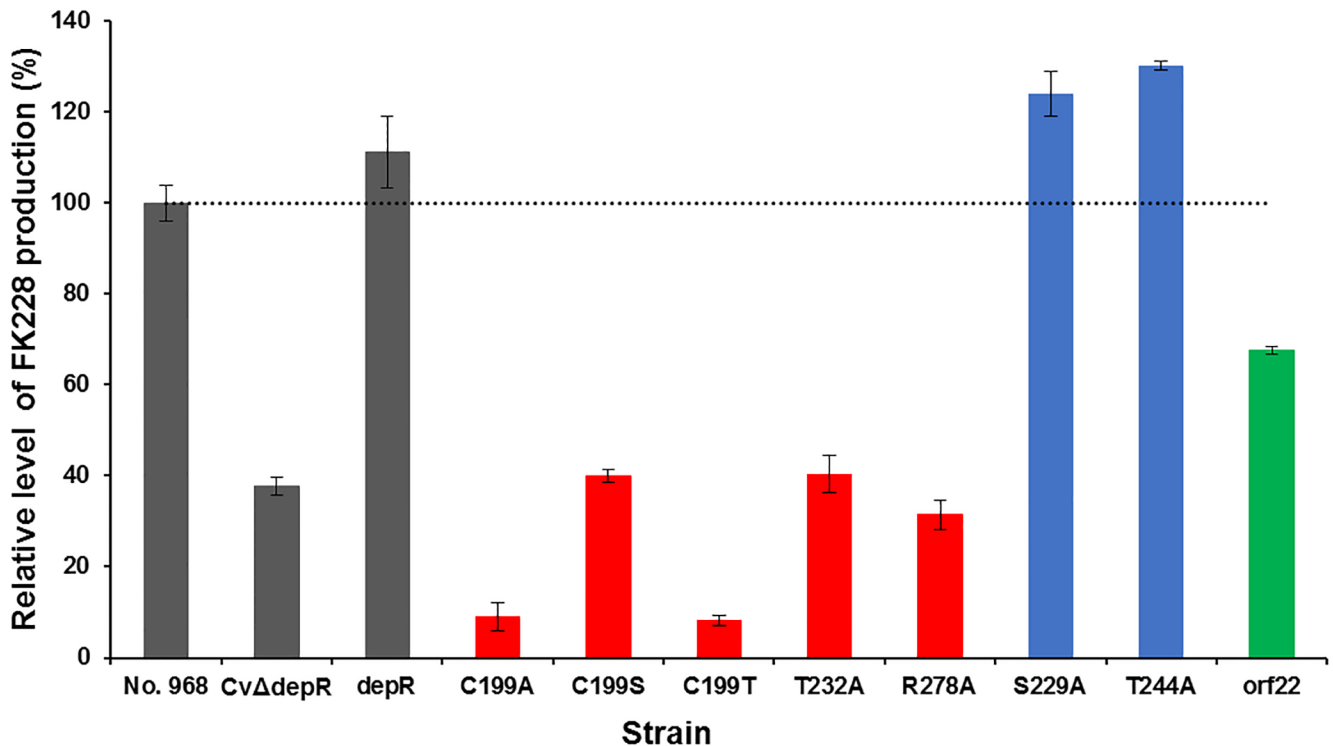


Fig 6. Relative levels of FK228 productions by *C. violaceum* strains detected and quantified by LC-MS. No. 968, the wild-type strain; CvΔdepR, *depR* gene deletion mutant strain. Eight complementation strains: *depR*, CvΔdepR (pBMTL-3-*depR*); C199A, CvΔdepR (pWHU3057); C199S, CvΔdepR (p3T9); C199T, CvΔdepR (pWHU3058); T232A, CvΔdepR (pWHU3060); R278A, CvΔdepR (pWHU3062); S299A, CvΔdepR (pWHU3059); T244A, CvΔdepR (pWHU3061). An overproduction strain of *orf22*, No. 968 (pWHU3070). Data are mean values of results from duplicate experiments with error bars indicating standard deviation (n = 3).

<https://doi.org/10.1371/journal.pone.0196173.g006>

suggest that the positive regulatory function of DepR on the biosynthesis of FK228 may be indirect.

Regulation of Min system and biosynthesis of polyhydroxyalkanoates (PHAs) by DepR

Polyhydroxyalkanoates (PHAs) are polyesters produced by numerous bacteria as carbon and energy storage compounds [41]. Phasins, PHA granule-associated proteins, promote PHA biosynthesis and affect the number and size of PHA granules [42]. Some *C. violaceum* strains are known to produce PHAs [43–46]. The observed repression of the expression of *orf22* encoding a phasin protein by DepR prompted us to propose that DepR regulates PHA biosynthesis through phasin protein Orf22. The Min system of cytokinesis is negatively related to PHA biosynthesis through DepR, since *depR* is the last gene of the putative *min* operon in *C. violaceum* (Fig 7).

GFP expression assays of P_{*orf21*} in the heterologous host *E. coli* suggested that DepR activates the putative *min* operon (Fig 4A), while the same result was not observed in the native host *C. violaceum* (Figs 4C and 5). This inconsistency may be due to the following one or two reasons. Firstly, the overexpression of *depR* in *E. coli* could have magnified or created an artificial regulatory effect of DepR. Secondly, there may be another layer of regulation of the putative *min* operon in the native host *C. violaceum*, which is absent in the heterologous host *E. coli*. In *Proteus mirabilis*, a member of the family Enterobacteriaceae, the transcription of

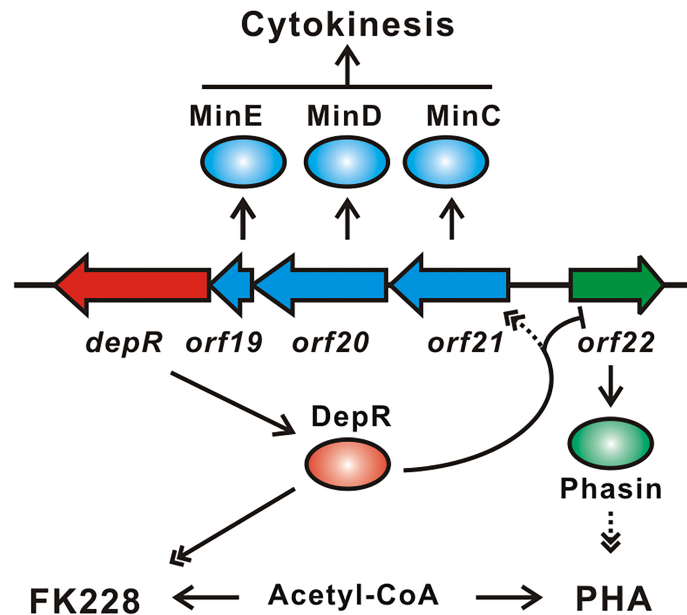


Fig 7. A model of regulation of cytokinesis, FK228 biosynthesis and PHA biosynthesis by DepR. The diagrams are defined as follows: arrow shapes, genes; ovals, proteins; lines with single arrow, biochemical reactions or life process; lines with double arrowheads, positive regulation; lines with a short bar, negative regulation; Dotted lines are predicted relationships without direct experimental data in *C. violaceum*.

<https://doi.org/10.1371/journal.pone.0196173.g007>

minCDE is positively regulated by RcsB, the response regulator of the Rcs phosphorelay two-component signal transduction system [47]. The DepR-binding site revealed in this study does not include the first LTTR-binding motif (Fig 1B, Motif I) that is conserved in the intergenic region upstream of *minC* in many other bacterial species. Motif I overlaps a 14-bp region (ATTGAAAGCCCGTC) which is consistent with the characterized RcsB-binding boxes (N₃-GA-N₅-C-N₃) in *E. coli* and *P. mirabilis* [48]. An RcsB homolog may regulate the transcription of the putative *min* operon in *C. violaceum* and interacts with DepR.

Since the transcription level of the putative *min* operon is not different in the wild-type No. 968 strain and the CvΔ*depR* mutant strain, we further probed the phasin protein gene *orf22*. Previous studies indicated that phasin proteins have an enhancing effect on PHA biosynthesis [49–53]. Gene *orf22* was inserted into pBMTL-3 to generate pWHU3070, which was transformed into No. 968, followed by fermentation and LC-MS. FK228 production in the *orf22*-overexpressed strain *C. violaceum* No.968 (pWHU3070) decreased by ca. 33% comparing to No. 968 (Fig 6, *orf22*). This observation promoted us to hypothesize that the enhancement of PHA biosynthesis induced by *orf22* overexpression may be one of reasons for a reduced production of FK228 in the CvΔ*depR* mutant. Because both FK228 biosynthesis and PHA biosynthesis utilize acetyl-CoA derivatives as building blocks, likely the two biosynthetic pathways have a competitive relationship for substrates (Fig 7).

Taken together, a possible model for gene regulation by DepR is shown in Fig 7, *depR* is co-transcribed with the putative *min* genes. DepR binds the intergenic region of the putative *minC* gene *orf21* and the putative phasin gene *orf22*, resulting in repression of *orf22* and activation of *orf21-20-19-depR*. As the phasin protein Orf22 reduces, PHA biosynthesis is downregulated and higher flux of acetyl-CoA derivatives is diverted towards FK228 biosynthesis. We also propose that DepR upregulates the transcription of FK228 biosynthetic genes through some other uncharacterized approaches.

Supporting information

S1 Table. Bacterial strains and plasmids used in this study.

(DOC)

S2 Table. Primers used in this study.

(DOC)

S1 Fig. SDS-PAGE analysis of recombinant His₆-DepR and His₆-DepR mutants.

(TIF)

S2 Fig. MALDI-TOF/TOF MS of recombinant His₆-DepR.

(TIF)

S3 Fig. DNA sequence of gene *orf21*, gene *orf22*, and the *orf21-orf22* intergenic region. The reverse complementary sequence of *orf21* is marked in pink (previously published) and blue (determined in this work). The *orf22* sequence (determined in this work) is marked in green. The start codons and stop codons of *orf21* and *orf22* are indicated by underlining. The *orf21-orf22* intergenic region is marked in red. The 77-bp DNA region bound by DepR is shown in bold. The sequence has been deposited in GenBank with Accession Number MG696726.

(PDF)

S4 Fig. GFP expression assays of the *minC* promoter of *E. coli* strain BL21(DE3).

(TIF)

S5 Fig. Identification of the DepR(C199S)-binding site in the *orf22-orf21* intergenic region using DIFA. The upper two electropherograms indicate the reactions in the absence of protein and the presence of 9.8 μg (6.8 μM) purified protein DepR(C199S). The lower electropherogram represents the sequencing reaction. The DNA sequence (black) shows DepR (C199S) binding sites.

(TIF)

S6 Fig. Effects of DTT and H₂O₂ on the binding of DepR to target DNA fragments. (A) EMSA analysis of DepR with target DNA fragments of DepR and 0–1.5 mM DTT. (B) EMSA analysis of DepR with target DNA fragments of DepR and 0–1.5 mM H₂O₂.

(TIF)

S7 Fig. EMSA analysis of DepR mutants with target DNA fragments of DepR. The bound DNA bands were indicated by yellow arrows.

(TIF)

S8 Fig. EMSA analysis of DepR with DNA fragments from *dep* gene cluster. (A) *dep* gene cluster, primer pairs and the sizes and locations of DNA fragments amplified using in EMSA. (B) EMSA analysis of DepR with DNA fragments.

(TIF)

Acknowledgments

We thank TOLO Biotechnology, Shanghai, China for assistance with DNase I footprinting assay.

Author Contributions

Conceptualization: Yongjian Qiao, Tiantian Tong, Yi-Qiang Cheng, Dongqing Zhu.

Data curation: Yongjian Qiao, Tiantian Tong, Yi-Qiang Cheng, Dongqing Zhu.

Formal analysis: Yongjian Qiao, Tiantian Tong, Jiao Xue, Wenjing Lin, Yi-Qiang Cheng, Dongqing Zhu.

Funding acquisition: Zixin Deng, Yi-Qiang Cheng, Dongqing Zhu.

Investigation: Yongjian Qiao, Tiantian Tong, Jiao Xue, Wenjing Lin, Yi-Qiang Cheng, Dongqing Zhu.

Methodology: Yongjian Qiao, Tiantian Tong, Jiao Xue, Yi-Qiang Cheng, Dongqing Zhu.

Project administration: Yi-Qiang Cheng, Dongqing Zhu.

Resources: Zixin Deng, Yi-Qiang Cheng, Dongqing Zhu.

Software: Yongjian Qiao, Yi-Qiang Cheng, Dongqing Zhu.

Supervision: Zixin Deng, Yi-Qiang Cheng, Dongqing Zhu.

Validation: Yongjian Qiao, Tiantian Tong, Jiao Xue, Wenjing Lin, Yi-Qiang Cheng, Dongqing Zhu.

Visualization: Yongjian Qiao, Tiantian Tong, Yi-Qiang Cheng, Dongqing Zhu.

Writing – original draft: Yongjian Qiao, Yi-Qiang Cheng, Dongqing Zhu.

Writing – review & editing: Yongjian Qiao, Yi-Qiang Cheng, Dongqing Zhu.

References

1. Rowlett VW, Margolin W. The Min system and other nucleoid-independent regulators of Z ring positioning. *Front Microbiol.* 2015; 6:478. <https://doi.org/10.3389/fmicb.2015.00478> PMID: 26029202.
2. Ortiz C, Natale P, Cueto L, Vicente M. The keepers of the ring: regulators of FtsZ assembly. *FEMS Microbiol Rev.* 2015; 40(1):57–67. <https://doi.org/10.1093/femsre/fuv040> PMID: 26377318.
3. Jia S, Keilberg D, Hot E, Thanbichler M, Sogaard-Andersen L, Lenz P. Effect of the Min system on timing of cell division in *Escherichia coli*. *PLoS One.* 2014; 9(8):e103863. <https://doi.org/10.1371/journal.pone.0103863> PMID: 25090009
4. de Boer PA, Crossley RE, Rothfield LI. Roles of MinC and MinD in the site-specific septation block mediated by the MinCDE system of *Escherichia coli*. *J Bacteriol.* 1992; 174(1):63–70. PMID: 1729224.
5. Hu Z, Lutkenhaus J. A conserved sequence at the C-terminus of MinD is required for binding to the membrane and targeting MinC to the septum. *Molecular microbiology.* 2003; 47(2):345–55. PMID: 12519187.
6. Loose M, Fischer-Friedrich E, Ries J, Kruse K, Schwille P. Spatial regulators for bacterial cell division self-organize into surface waves *in vitro*. *Science.* 2008; 320(5877):789–92. <https://doi.org/10.1126/science.1154413> PMID: 18467587.
7. Parti RP, Horbay MA, Liao M, Dillon JA. Regulation of *minD* by *oxyR* in *Neisseria gonorrhoeae*. *Res Microbiol.* 2013; 164(5):406–15. <https://doi.org/10.1016/j.resmic.2013.02.002> PMID: 23434849.
8. Ueda H, Nakajima H, Hori Y, Fujita T, Nishimura M, Goto T, et al. FR901228, a novel antitumor bicyclic depsipeptide produced by *Chromobacterium violaceum* No. 968. I. Taxonomy, fermentation, isolation, physico-chemical and biological properties, and antitumor activity. *J Antibiot (Tokyo).* 1994; 47(3):301–10. PMID: 7513682.
9. Ueda H, Nakajima H, Hori Y, Goto T, Okuhara M. Action of FR901228, a novel antitumor bicyclic depsipeptide produced by *Chromobacterium violaceum* no. 968, on Ha-ras transformed NIH3T3 cells. *Biosci Biotechnol Biochem.* 1994; 58(9):1579–83. PMID: 7765477.
10. Nakajima H, Kim YB, Terano H, Yoshida M, Horinouchi S. FR901228, a potent antitumor antibiotic, is a novel histone deacetylase inhibitor. *Exp Cell Res.* 1998; 241(1):126–33. <https://doi.org/10.1006/excr.1998.4027> PMID: 9633520.
11. Furumai R, Matsuyama A, Kobashi N, Lee KH, Nishiyama M, Nakajima H, et al. FK228 (depsipeptide) as a natural prodrug that inhibits class I histone deacetylases. *Cancer Res.* 2002; 62(17):4916–21. PMID: 12208741.

12. Cheson BD, Horwitz SM, Weisenburger DD. Peripheral T-cell lymphomas: diagnosis and treatment options. Proceedings from a live roundtable, August 17, 2011, Kauai, Hawaii. Clin Adv Hematol Oncol. 2011; 9(11 Suppl 26):1–14; quiz 5–6. PMID: [22362328](#).
13. VanderMolen KM, McCulloch W, Pearce CJ, Oberlies NH. Romidepsin (Istodax, NSC 630176, FR901228, FK228, depsipeptide): a natural product recently approved for cutaneous T-cell lymphoma. J Antibiot (Tokyo). 2011; 64(8):525–31. <https://doi.org/10.1038/ja.2011.35> PMID: [21587264](#).
14. Gong F, Chiu LY, Miller KM. Acetylation Reader Proteins: Linking Acetylation Signaling to Genome Maintenance and Cancer. PLoS genetics. 2016; 12(9):e1006272. <https://doi.org/10.1371/journal.pgen.1006272> PMID: [27631103](#)
15. Cheng YQ, Yang M, Matter AM. Characterization of a gene cluster responsible for the biosynthesis of anticancer agent FK228 in *Chromobacterium violaceum* No. 968. Appl Environ Microbiol. 2007; 73(11):3460–9. <https://doi.org/10.1128/AEM.01751-06> PMID: [17400765](#).
16. Wang C, Wesener SR, Zhang H, Cheng YQ. An FAD-dependent pyridine nucleotide-disulfide oxidoreductase is involved in disulfide bond formation in FK228 anticancer depsipeptide. Chem Biol. 2009; 16(6):585–93. <https://doi.org/10.1016/j.chembiol.2009.05.005> PMID: [19549597](#).
17. Potharla VY, Wesener SR, Cheng YQ. New insights into the genetic organization of the FK228 biosynthetic gene cluster in *Chromobacterium violaceum* no. 968. Appl Environ Microbiol. 2011; 77(4):1508–11. <https://doi.org/10.1128/AEM.01512-10> PMID: [21183645](#).
18. Wesener SR, Potharla VY, Cheng YQ. Reconstitution of the FK228 biosynthetic pathway reveals cross talk between modular polyketide synthases and fatty acid synthase. Appl Environ Microbiol. 2011; 77(4):1501–7. <https://doi.org/10.1128/AEM.01513-10> PMID: [21183648](#).
19. Sambrook J, Fritsch E. F., and Maniatis T. Molecular cloning: a laboratory manual. ed n, editor. Cold Spring Harbor, N.Y.: Cold Spring Harbor Laboratory; 1989.
20. Bradford MM. A rapid and sensitive method for the quantitation of microgram quantities of protein utilizing the principle of protein-dye binding. Anal Biochem. 1976; 72:248–54. PMID: [942051](#).
21. Broetto L, Cecagno R, Sant'anna FH, Weber S, Schrank IS. Stable transformation of *Chromobacterium violaceum* with a broad-host-range plasmid. Applied microbiology and biotechnology. 2006; 71(4):450–4. <https://doi.org/10.1007/s00253-005-0140-5> PMID: [16172890](#).
22. Wennerhold J, Krug A, Bott M. The AraC-type regulator RipA represses aconitase and other iron proteins from *Corynebacterium* under iron limitation and is itself repressed by DtxR. J Biol Chem. 2005; 280(49):40500–8. <https://doi.org/10.1074/jbc.M508693200> PMID: [16179344](#).
23. Bussmann M, Baumgart M, Bott M. RosR (Cg1324), a hydrogen peroxide-sensitive MarR-type transcriptional regulator of *Corynebacterium glutamicum*. J Biol Chem. 2010; 285(38):29305–18. <https://doi.org/10.1074/jbc.M110.156372> PMID: [20643656](#).
24. Zhu D, Wang Y, Zhang M, Ikeda H, Deng Z, Cane DE. Product-mediated regulation of pentalenolactone biosynthesis in *Streptomyces* species by the MarR/SlyA family activators PenR and PntR. J Bacteriol. 2013; 195(6):1255–66. <https://doi.org/10.1128/JB.02079-12> PMID: [23316039](#).
25. Davis JR, Brown BL, Page R, Sello JK. Study of PcaV from *Streptomyces coelicolor* yields new insights into ligand-responsive MarR family transcription factors. Nucleic acids research. 2013; 41(6):3888–900. <https://doi.org/10.1093/nar/gkt009> PMID: [23396446](#)
26. Wang Y, Cen XF, Zhao GP, Wang J. Characterization of a new GlnR binding box in the promoter of *amtB* in *Streptomyces coelicolor* inferred a PhoP/GlnR competitive binding mechanism for transcriptional regulation of *amtB*. J Bacteriol. 2012; 194(19):5237–44. <https://doi.org/10.1128/JB.00989-12> PMID: [22821977](#).
27. Pescaretti Mde L, Lopez FE, Morero RD, Delgado MA. Transcriptional autoregulation of the RcsCDB phosphorelay system in *Salmonella enterica* serovar Typhimurium. Microbiology. 2010; 156(Pt 12):3513–21. <https://doi.org/10.1099/mic.0.041319-0> PMID: [20724387](#).
28. Kalir S, Mangan S, Alon U. A coherent feed-forward loop with a SUM input function prolongs flagella expression in *Escherichia coli*. Molecular systems biology. 2005; 1:2005 0006. <https://doi.org/10.1038/msb4100010> PMID: [16729041](#)
29. Livak KJ, Schmittgen TD. Analysis of relative gene expression data using real-time quantitative PCR and the 2⁻(Delta Delta C(T)) Method. Methods. 2001; 25(4):402–8. <https://doi.org/10.1006/meth.2001.1262> PMID: [11846609](#).
30. Seo SW, Kim D, Szubin R, Palsson BO. Genome-wide Reconstruction of OxyR and SoxRS Transcriptional Regulatory Networks under Oxidative Stress in *Escherichia coli* K-12 MG1655. Cell Rep. 2015; 12(8):1289–99. <https://doi.org/10.1016/j.celrep.2015.07.043> PMID: [26279566](#).
31. Toledano MB, Kullik I, Trinh F, Baird PT, Schneider TD, Storz G. Redox-dependent shift of OxyR-DNA contacts along an extended DNA-binding site: a mechanism for differential promoter selection. Cell. 1994; 78(5):897–909. PMID: [8087856](#).

32. Reen FJ, Haynes JM, Mooij MJ, O'Gara F. A non-classical LysR-type transcriptional regulator PA2206 is required for an effective oxidative stress response in *Pseudomonas aeruginosa*. *PLoS One*. 2013; 8(1):e54479. <https://doi.org/10.1371/journal.pone.0054479> PMID: 23382903
33. Panmanee W, Charoenlap N, Atichartpongkul S, Mahaviahakanont A, Whiteside MD, Winsor G, et al. The OxyR-regulated *phnW* gene encoding 2-aminoethylphosphonate:pyruvate aminotransferase helps protect *Pseudomonas aeruginosa* from tert-butyl hydroperoxide. *PLoS One*. 2017; 12(12):e0189066. <https://doi.org/10.1371/journal.pone.0189066> PMID: 29216242.
34. Jo I, Chung IY, Bae HW, Kim JS, Song S, Cho YH, et al. Structural details of the OxyR peroxide-sensing mechanism. *Proc Natl Acad Sci U S A*. 2015; 112(20):6443–8. <https://doi.org/10.1073/pnas.1424495112> PMID: 25931525
35. Hillion M, Antelmann H. Thiol-based redox switches in prokaryotes. *Biological chemistry*. 2015; 396(5):415–44. <https://doi.org/10.1515/hsz-2015-0102> PMID: 25720121
36. Vazquez-Torres A. Redox active thiol sensors of oxidative and nitrosative stress. *Antioxidants & redox signaling*. 2012; 17(9):1201–14. <https://doi.org/10.1089/ars.2012.4522> PMID: 22257022
37. Wang X, Mukhopadhyay P, Wood MJ, Outten FW, Opydyke JA, Storz G. Mutational analysis to define an activating region on the redox-sensitive transcriptional regulator OxyR. *J Bacteriol*. 2006; 188(24):8335–42. <https://doi.org/10.1128/JB.01318-06> PMID: 17012382
38. Wang C, Henkes LM, Doughty LB, He M, Wang D, Meyer-Almes FJ, et al. Thailandepsins: bacterial products with potent histone deacetylase inhibitory activities and broad-spectrum antiproliferative activities. *J Nat Prod*. 2011; 74(10):2031–8. <https://doi.org/10.1021/np200324x> PMID: 21793558.
39. Potharla VY, Wang C, Cheng YQ. Identification and characterization of the spiruchostatin biosynthetic gene cluster enable yield improvement by overexpressing a transcriptional activator. *J Ind Microbiol Biotechnol*. 2014; 41(9):1457–65. <https://doi.org/10.1007/s10295-014-1474-8> PMID: 24973954.
40. Biggins JB, Gleber CD, Brady SF. Acyldepsipeptide HDAC inhibitor production induced in *Burkholderia thailandensis*. *Org Lett*. 2011; 13(6):1536–9. <https://doi.org/10.1021/ol200225v> PMID: 21348454.
41. Koller M. Advances in Polyhydroxyalkanoate (PHA) Production. *Bioengineering*. 2017; 4(4). <https://doi.org/10.3390/bioengineering4040088> PMID: 29099065.
42. Mezzina MP, Pettinari MJ. Phasins, Multifaceted Polyhydroxyalkanoate Granule-Associated Proteins. *Appl Environ Microbiol*. 2016; 82(17):5060–7. <https://doi.org/10.1128/AEM.01161-16> PMID: 27287326
43. Steinbüchel A, Debzi E-M, Marchessault RH, Timm A. Synthesis and production of poly(3-hydroxyvaleric acid) homopolyester by *Chromobacterium violaceum*. *Applied microbiology and biotechnology*. 1993; 39(4):443–9. <https://doi.org/10.1007/bf00205030>
44. Kolibachuk D, Miller A, Dennis D. Cloning, molecular analysis, and expression of the polyhydroxyalkanoic acid synthase (*phaC*) gene from *Chromobacterium violaceum*. *Appl Environ Microbiol*. 1999; 65(8):3561–5. PMID: 10427049
45. Bhubalan K, Chuah JA, Shozui F, Brigham CJ, Taguchi S, Sinskey AJ, et al. Characterization of the highly active polyhydroxyalkanoate synthase of *Chromobacterium* sp. strain USM2. *Appl Environ Microbiol*. 2011; 77(9):2926–33. <https://doi.org/10.1128/AEM.01997-10> PMID: 21398494
46. Ling SC, Tsuge T, Sudesh K. Biosynthesis of novel polyhydroxyalkanoate containing 3-hydroxy-4-methylvalerate by *Chromobacterium* sp. USM2. *Journal of applied microbiology*. 2011; 111(3):559–71. <https://doi.org/10.1111/j.1365-2672.2011.05084.x> PMID: 21689225.
47. Howery KE, Clemmer KM, Simsek E, Kim M, Rather PN. Regulation of the Min Cell Division Inhibition Complex by the Rcs Phosphorelay in *Proteus mirabilis*. *J Bacteriol*. 2015; 197(15):2499–507. <https://doi.org/10.1128/JB.00094-15> PMID: 25986901
48. Howery KE, Clemmer KM, Rather PN. The Rcs regulon in *Proteus mirabilis*: implications for motility, biofilm formation, and virulence. *Current genetics*. 2016; 62(4):775–89. <https://doi.org/10.1007/s00294-016-0579-1> PMID: 26936153.
49. Ushimaru K, Motoda Y, Numata K, Tsuge T. Phasin proteins activate *Aeromonas caviae* polyhydroxyalkanoate (PHA) synthase but not *Ralstonia eutropha* PHA synthase. *Appl Environ Microbiol*. 2014; 80(9):2867–73. <https://doi.org/10.1128/AEM.04179-13> PMID: 24584238
50. Fukui T, Kichise T, Iwata T, Doi Y. Characterization of 13 kDa granule-associated protein in *Aeromonas caviae* and biosynthesis of polyhydroxyalkanoates with altered molar composition by recombinant bacteria. *Biomacromolecules*. 2001; 2(1):148–53. PMID: 11749166.
51. Tian SJ, Lai WJ, Zheng Z, Wang HX, Chen GQ. Effect of over-expression of phasin gene from *Aeromonas hydrophila* on biosynthesis of copolyesters of 3-hydroxybutyrate and 3-hydroxyhexanoate. *FEMS microbiology letters*. 2005; 244(1):19–25. <https://doi.org/10.1016/j.femsle.2005.01.020> PMID: 15727816.

52. York GM, Stubbe J, Sinskey AJ. New insight into the role of the PhaP phasin of *Ralstonia eutropha* in promoting synthesis of polyhydroxybutyrate. *J Bacteriol.* 2001; 183(7):2394–7. <https://doi.org/10.1128/JB.183.7.2394-2397.2001> PMID: 11244085
53. York GM, Stubbe J, Sinskey AJ. The *Ralstonia eutropha* PhaR protein couples synthesis of the PhaP phasin to the presence of polyhydroxybutyrate in cells and promotes polyhydroxybutyrate production. *J Bacteriol.* 2002; 184(1):59–66. <https://doi.org/10.1128/JB.184.1.59-66.2002> PMID: 11741844